Envisioning enhanced composite structures using graphene coated fibre optical sensor

D. SAVASTRU, I. S. DONTU*, V. SAVU, D. TENCIU, A. STANCIU
National Institute R&D of Optoelectronics INOE 2000, 409 Atomistilor Str., Magurele, 077125 Ilfov, Romania

We report simulation of a fibre optic sensors class of potential interest for various applications, namely Long Period Grating Fibre Sensors (LPGFS) having a graphene layer deposited on the cladding in the grating zone. Studied LPGFS consists of single mode (SM) fused silica optical fibre onto/into which a grating with 10 µm to 1000 µm is inscribed over a 5 mm to 75 mm length zone. During the simulations, the main issue of interest is the displacement of peak wavelengths and bandwidths broadening of the absorption bands corresponding to the energy transfer from core propagating mode to the possible cladding modes at the interaction with the grating as results of ambient medium different factors action.

1. Introduction

The integration of graphene-coated fibre optic sensors into composite structures represents a transformative advancement in structural health monitoring (SHM). With the increasing demand for durable, lightweight, and intelligent materials in aerospace, civil infrastructure, and automotive industries, the need for real-time, highly sensitive, and multifunctional sensing capabilities has never been greater.

Graphene, a single layer of carbon atoms arranged in a hexagonal lattice, exhibits extraordinary mechanical, electrical, and thermal properties. When applied as a coating on fibre optic sensors, graphene enhances their sensitivity, durability, and multifunctionality, enabling them to detect a wide range of parameters, including strain, temperature, pressure, and chemical composition.

By leveraging the unique properties of graphene and integrating them with fibre optic sensing techniques, researchers and engineers are paving the way for next-generation composite materials with self-sensing and self-healing capabilities. These advancements hold immense promise for improving the longevity, safety, and efficiency of critical structures across various engineering domains. This approach leverages the exceptional properties of graphene—such as high electrical conductivity, mechanical strength, and thermal stability—to enhance the performance of fibre optic sensors embedded within composite materials [1-3]. Recent developments have focused on creating nanocomposite coatings that combine graphene oxide with polymide for optical fibres.

Different sensors are used in SHM systems to monitor composite structures. Most common sensors are strain gauges, fibre Bragg grating sensors (FBGs), and piezoelectric transducers used to establish either an elastic ultrasonic wave in-situ inspection method or an acoustic emissions-based inspection method. Additionally, graphene-based materials have been integrated into various optical fiber sensor configurations, including interferometry-based sensors, surface plasmon resonance (SPR) sensors, and absorption-based sensors. These integrations have enhanced sensitivity and selectivity for detecting gases, chemicals, and biological species [4 -11].

Among other techniques, optical fibre sensing is of large interest for health monitoring of composite structures because of its fibrous nature and multiaxial sensitivity of optical fibre [12-25].

Also there are absolutely necessary continuous determination of composites structure chemical status in the sense of detecting infestation with various impurities.

One of their main features is that the optical fibre itself can act as both the transmission medium and the transducer, hence allowing remote sensing and multiplexing. Additionally, optical fibre sensors are light and small, resistant to harsh environments and high temperatures, biocompatible, immune to electromagnetic fields and electromagnetically passive [26-28].

In this paper we report simulation/design of a fibre optic sensors class of potential interest for various applications, namely Long Period Grating Fibre Sensors (LPGFS) having a graphene layer deposited on the cladding in the grating zone. Graphene is a two-dimensional (2D) material with only one carbon atom thickness. Graphene is considerate a the "material of the future," because of its multiple applications in different sectors with remarkable mechanical, electrical, optical, and biological properties [29].

There is a large and progressive production of different graphene materials (GO, rGO, fGO, frGO and mG) with particular focus on specific applications and this is expected to be continued for at least a couple of decades as it is meeting promising applications and requirements. Studied LPGFS consists of single mode (SM) fused silica optical fibre onto/into which a grating with 10 µm to 1000

µm is inscribed over a 5 mm to 75 mm length zone. In this zone the PMMA protection layer is removed creating a direct contact of the optic fibre with the ambient medium. The sensing capabilities of LPGFS are greatly improved by deposition of a graphene (G) layer, a two-dimensional carbon material on this optic fibre cladding zone. During the simulations, the main issue of interest is the displacement of peak wavelengths and bandwidths broadening of the absorption bands corresponding to the energy transfer from core propagating mode to the possible cladding modes at the interaction with the grating as results of ambient medium different factors action. The ambient medium can be the epoxy resin layer of a composite material or the joint of two structure parts made of composite. During the simulations a special care was dedicated to investing the role of graphene layer thickness from one-atom-thickness up to 400 nm. There were analysed the cases of the three main types of graphene commercially available, namely graphene (G), graphene oxide (GO) and reduced graphene oxide (rGO).

2. Composites structures health monitoring- theory

The theory of composite material health is grounded in understanding the behavior and response of composite structures under various loading conditions. This includes how damage propagates, how external loads interact with the material properties, and how these changes affect the overall performance of the structure.

Optical Fibre Bragg Grating (FBG) Sensors are integrated into graphene Fibre optics for precise strain and temperature measurements. The principle is based on the reflection of a specific wavelength of light from a grating in the Fibre, which shifts when the fibre undergoes strain or temperature changes. By embedding graphene FBG sensors into composite materials, structural changes such as strain, displacement, or temperature changes can be continuously monitored with high spatial resolution.

Since 1995, optic fibres gained importance as sensors, particularly as biochemical sensors. Among optic fibre sensors, Long Period Grating Fibre Sensors (LPGFS) and/or Tilted Fibre Bragg Grating (TFBG) begun to be more and more used for detection of various chemicals. The main feature of LPGFS and/or TFBG which made them of increasing interest for chemical detection is that in the grating zone the standard mechanical protection epoxy acrylate fibre coating is removed putting the cladding surface in direct contact with the ambient [30 -33].

Normally, an infinitesimal modification of the water refractive index can be detected with the LPGFS which works as a refractometer. A LPGFS consists of a single mode (SM) optical fibre basically used as a light propagation guide into and from the sensing zone and which is processed by inscribing a diffraction Bragg grating into it. One important feature of the LPG is that the grating zone of the host optical fibre is placed in direct contact with the ambient and can be directly affected by the microscale possible changes of ambient measured by

refractive index variations. The LPGFS operation relies on observing the spectral broadenings and shifts of the absorption bands induced by the Bragg grating scattering in the optical fibre transmission spectrum. The absorption bands are induced by the coupling process between the fundamental mode propagating through the optical fibre core and the modes propagating through the fibre cladding. The peaks of the absorption bands correspond to the Bragg resonance wavelengths of the LPG.

This configuration, where $n_3 > n_1 > n_2 > n_{ai}{}^r$, is commonly used to enhance the coupling efficiency and sensitivity of LPG sensors.

```
+------------------------------+
|        Thin-Film             |
|        Coating (n3)          |
+------------------------------+
|       Fibre Cladding         |
|          (n2)                |
+------------------------------+
|        Fibre Core            |
|          (n1)                |
+------------------------------+
|        Air (nair)            |
```
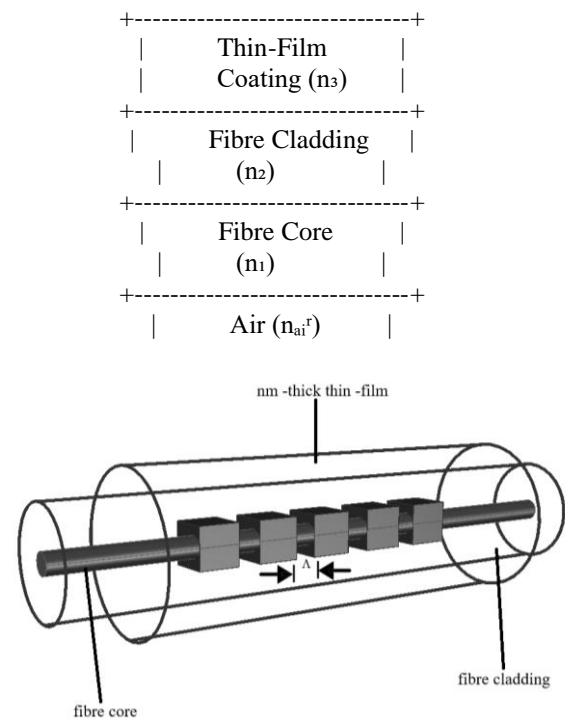

Fig. 1. Illustrative schematic of LPG with a nm-thick thin-film coating

- Fibre Core (n_1): The central region of the optical fibre, where light is primarily guided.
- Fibre Cladding (n_2): Surrounds the core and has a lower refractive index, ensuring total internal reflection within the core.
- Thin-Film Coating (n_3): An additional layer applied to the cladding, often with a refractive index higher than both the core and cladding. This layer can enhance the coupling between core modes and cladding modes, improving sensor performance.
- Air ($n_{ai}{}^r$): The external environment surrounding the fibre, typically having a refractive index of approximately 1.

This layered structure allows for efficient coupling of light from the core to the cladding modes, which is essential for the functionality of LPG-based sensors. The thin-film coating, with its higher refractive index, facilitates this coupling by creating a graded refractive

index profile that matches the core and cladding modes more effectively.

LPGFS provide an attractive platform for building optical sensors, because are more robust, cheaper, simpler to use and allows proper designs of portable devices. The structure of LPGFS allows important functional improvements by using layer-by-layer deposition technique for building nanoscale thin films on outer surface in the zone where the diffraction Bragg grating is inscribed. The LPGFS are operated observing the absorption bands induced by the grating scattering in the fibre transmission spectrum. The LPGFS exploits the coupling process between the propagating through the fibre core mode and the modes propagating through the fibre cladding. The whole process is produced into the optical fibre placed in direct contact with the ambient and can be directly affected by the microscale possible changes of the ambient measured by refractive index variations.

The net, measurable effect of this light energy transfer consists in appearance of several absorption bands with well-defined peak wavelength and bandwidths in the broadband spectrum of the fundamental mode propagating through the core. It can be theoretically justified that the values of the absorption bands peak wavelengths and bandwidths depend on the fibre optic core and cladding diameters and on the core, cladding and ambient environment refractive indexes. In the cases of biological and chemical applications, the inner geometry of the LPGFS being kept unchanged any modification of ambient-index change produces shifts absorption bands peak wavelengths correlated with bandwidths broadenings. An ambient-index change of $\sim 10^{-4}$ can be detected [34 – 36].

Assuming perfect bonding between the optical fibre sensors and the surrounding host material, axial strains are almost perfectly transferred from the host to the sensor, allowing a direct readout of axial strain from the sensor response.

However, when multiaxial sensing is envisaged, one must account for the differences in stiffness between the host material and the optical fibre sensor (and optionally its coating).

Fibre optic sensors use a 3-axis system, and the 1′-2′ (x, y) axis are perpendicular to the fibre.

LPGFS operation is described by the Eq. (1) for which there is no analytical solution [37, 38]:

$$\lambda_l^{(i)} = (n_{eff}(\lambda^{(i)} - n_{clad}^{(l)}(\lambda^{(i)}))\Lambda_{LPG} \qquad (1)$$

where $\lambda^{(i)}$ is the wavelength of the light signal injected in the core of the SM optic fibre with:

n_{eff} is the effective value of the core refraction index

n_{clad} is the refractive index effective value corresponding to the possible light cladding co-propagating mode l

Λ_{LPG} is the grating spatial period modulation.

This equation describes how light at specific wavelengths λ^i couples from the core mode into specific cladding modes in an LPG structure. The resonance occurs when the difference between the effective indices of the core mode and a cladding mode matches the periodic modulation induced by the grating.

Assuming a linear material response and small deformations of the composite, the strain transfer can be described in its most general form through the use of a transfer coefficient (TC) matrix, defined as:

$$\begin{bmatrix} \varepsilon_1^c \\ \varepsilon_2^c \\ \vdots \\ \varepsilon_6^c \\ \Delta T^c \end{bmatrix} = \begin{bmatrix} TC_{11} & TC_{12} & \dots & TC_{16} & TC_{17} \\ TC_{21} & TC_{22} & & TC_{26} & TC_{27} \\ \vdots & & \ddots & & \vdots \\ TC_{61} & TC_{62} & \dots & TC_{66} & TC_{67} \\ TC_{71} & TC_{72} & & TC_{76} & TC_{77} \end{bmatrix} \begin{bmatrix} \varepsilon_1^s \\ \varepsilon_2^s \\ \vdots \\ \varepsilon_6^s \\ \Delta T^s \end{bmatrix}$$

where: ε^c refers to far-field strains measured in the composite host.

ε^s refers to the strain field in the FBG sensor core;

ΔT is the change in temperature (which will affect the strain transfer as a result of differences in composite structures).

TC_{ij} represent the transfer coefficients between the sensor and the host (composite) strains

A Transfer Coefficient Matrix (TCM) is a mathematical construct used to model and analyze the relationships between multiple inputs and outputs in a system. It is particularly useful in fields such as control systems, fluid dynamics, and environmental modeling, where systems exhibit multiple interacting components. In a system with multiple inputs and outputs, the TCM is represented as a matrix that maps each input to its corresponding output. For a system with n inputs and m outputs, the TCM is an m×n matrix, where each element Tij represents the influence of input i on output j.

A LPGFS is a type of optic fibre device consisting of an single mode (SM) optic fibre in the core of which a low amplitude spatially modulation of core refraction index is created by various fabrication methods, the most common being the controlled thermal processing using a low/medium CO_2 laser. Ours LPGFS consists of single mode (SM) fused silica optical fibre onto/into which a grating with 10 mm to 1000 mm period is inscribed over a 5 mm to 75 mm length zone. In this zone the PMMA (PolyMethylMethAcrylate) protection layer is removed creating a direct contact of the optic fibre with the ambient medium.

The sensing capabilities of LPGFS are greatly improved by deposition of a graphene (G) layer, a two-dimensional carbon material on this optic fibre cladding zone.

During the simulations, the main issue of interest is the displacement of peak wavelengths and bandwidths broadening of the absorption bands corresponding to the energy transfer from core propagating mode to the possible cladding modes at the interaction with the grating as results of ambient medium different factors action.

The ambient medium can be the epoxy resin layer of a composite material or the joint of two structure parts made of composite.

During the simulations a special care was dedicated to investing the role of graphene layer thickness from one-atom-thickness up to 400 nm for three main types of graphene commercially available, namely graphene (G), graphene oxide (GO) and reduced graphene oxide (rGO).

3. Simulation results

In this paper simulations are performed using a coordinate system defined as:

The 1-direction corresponds to the fibre reinforcement direction;

The 2-direction is perpendicular to the reinforcements & the layer;

The 3-direction is the out-of-plane transverse direction.

LPGFS simulation is accomplished in 3 stages.

In the first stage n_{eff} are calculated. In Fig. 2 the plot represents the dispersion characteristics of an optical fibre, showing how the effective refractive index of the core and various cladding modes change with wavelength. The calculated values are introduced into Eq. 1 for the stage of simulation.

The topmost curve (blue) represents the core refractive index, which decreases as the wavelength increases. This is typical because, in optical fibres, the refractive index of the core generally decreases with increasing wavelength due to material dispersion.

Several other curves below it represent different cladding modes labeled as "Clad Mode 1," "Clad Mode 2," and so on up to "Clad Mode 9." The first 9 cladding modes (the lower curves) also show a decreasing trend but at different rates. These modes represent light propagating within the cladding rather than the core.

The decreasing trend suggests normal dispersion behavior, where the refractive index decreases as wavelength increases. The gap between the core and cladding modes indicates how light coupling occurs in a Long-Period Grating Fibre Sensor (LPGFS). When the fundamental core mode couples into a cladding mode at specific wavelengths, it results in attenuation dips in the transmission spectrum, which are useful for sensing applications. The dispersion behavior of these modes is crucial for designing optical fibre sensors and communication devices, as it determines how light interacts with the fibre and external perturbations like temperature, strain, and surrounding refractive index.
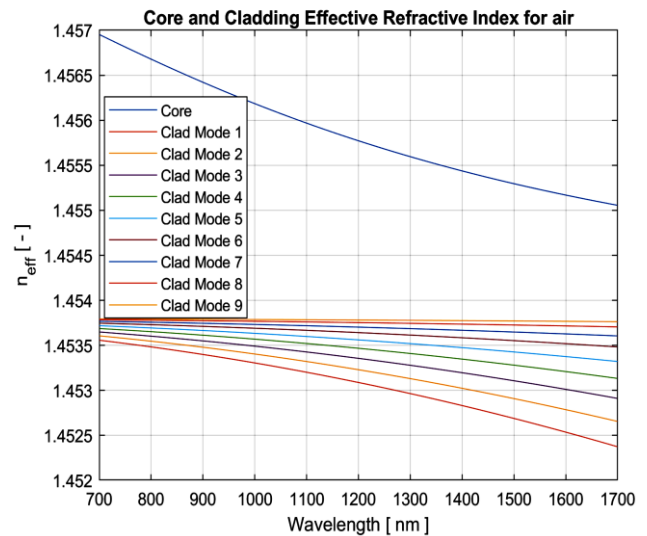
Fig. 2. Core and cladding Effective Refractive Index Values vs Wavelength simulated for LPGFS (colour online)

The graph 3 represents results obtained in the second simulation stage namely Phase Matching Curves for air (PMC), showing the relationship between the wavelength (nm) on the x-axis and Λ_{LPG} (μm) on the y-axis for different modes. All the curves exhibit a monotonic increasing trend, meaning Λ_{LPG} increases as the wavelength increases. The curves become more widely spaced at higher wavelengths, indicating a non-linear relationship between Λ_{LPG} and wavelength. As the mode number increases, the corresponding Λ_{LPG} values increase for the same wavelength. The shape of the curves suggests a non-linear, possibly exponential increase in Λ_{LPG} with increasing wavelength.

PMC are parametric curves formed by pairs (wavelength – grating period) for which the Bragg resonance condition is fulfilled. Bragg resonance condition is the maximum energy transfer from the core mode to the clad-ding modes when interacting with the grating. The PMC of the investigated LPGFS is represented in a coordinate system (wavelength - LPG period, denoted as Λ_{LPG}). In Fig. 4 it can be noticed that a line corresponding to Λ_{LPG} of 775 μm and parallel to wavelength axis intersects the PMC in 7 points corresponding to Modes 1 to 7. These intersection points correspond each to a $\lambda_{(i)}$ value. There are kept only the first seven Modes because higher ones correspond to $\lambda_{(i)}$ situated outside the spectral range of interest. Because of a higher accuracy, the simulations were accomplished using an analytical method of $\lambda_{(i)}$ calculation not a graphical one. The results obtained for Core & Cladding (first 9 possible) modes are presented in the graph.
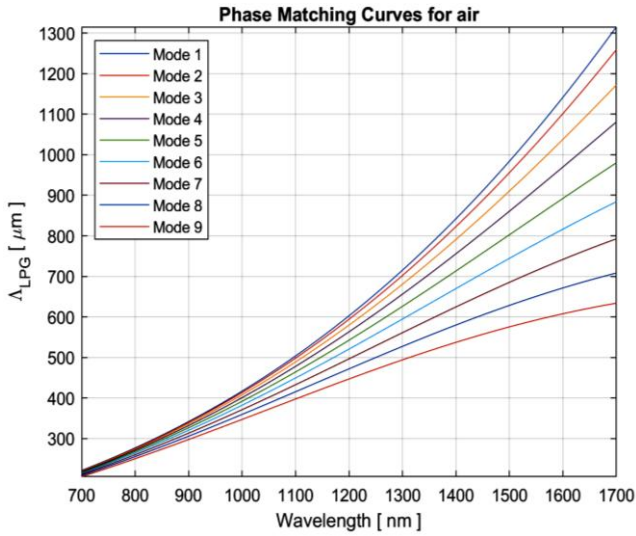
Fig. 3. Phase Matching curves for air (colour online)

Fig. 4. The simulated transmission spectrum of the investigated LPGFS

The graph 4 represents the LPG (Long-Period Grating) Transmission Spectrum for Λ_{LPG} = 775 μm in the next simulation stage. The blue curve shows multiple deep dips at different wavelengths. These dips indicate resonance wavelengths where light is coupled from the core mode to cladding modes, leading to attenuation. The dips correspond to specific mode numbers (Mode 2, Mode 3, etc.). Each labeled mode represents a particular resonance condition. Lower-order modes (Mode 2, Mode 3, etc.) appear at shorter wavelengths. Higher-order modes (Mode 6, Mode 7, etc.) appear at longer wavelengths. This is consistent with phase matching conditions in LPGs. The deepest dip appears around 1650 nm (Mode 7). This suggests stronger coupling and higher energy transfer to this mode at this wavelength. This spectrum shows the wavelengths at which LPG induces mode coupling, leading to attenuation. The resonance wavelengths depend on grating period (Λ_{LPG}), refractive index profile, and surrounding medium.

Also in Fig. 4 it can be observed that the absorption Bragg resonance bands have decreasing intensities corresponding to inverse modes order. This is caused because the mode denomination used in the computer simulation algorithm. The LPGFS use is based on determining the spectral shifts of the absorption spectra when ambient refractive index changes. In Fig. 5 the modes having longer resonance wavelength are the ones for which the Bragg resonance condition is easier accomplished. These are the cladding modes which propagate closer to the optic fibre axis.

Fig. 5 presents the transmission spectrum of Mode 6. Its peak Bragg resonance wavelength is situated at λ_{res} = 1541.95 nm. This is the resonance wavelength where maximum power is coupled from the core mode to Mode 6, leading to attenuation. The resonance at 1541.95 nm can be used for applications like wavelength-selective filtering, fibre sensing (e.g., temperature, strain, refractive index sensing), or telecommunications

Mode 6 was chosen because its λ_{res} is placed near the middle of the LPGFS interrogator input spectral domain. A Mode 6 spectral shift appears as a result of bending or stress induced by composite strain.

The transmission spectrum has a symmetrical shape, resembling a Gaussian or Lorentzian profile. This indicates a well-defined resonance with a relatively narrow bandwidth. Any shift in the resonance wavelength (λ_{res}) can indicate external perturbations, making LPGs useful for sensing applications.
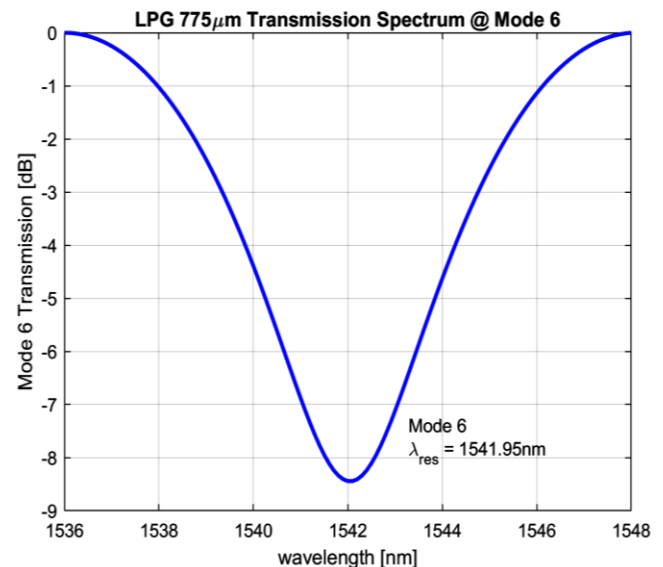
Fig. 5. LPG 775 μm Transmission Spectrum @ Mode 6

In stage 3 we simulated the spectral shifts of Modes 1 to 7 absorption band peaks when a Composite combined longitudinal and bending strain is applied on LPGFS. The graph 6 show how different resonance mode shift with increasing strain. Mode 7 shift (black line) shows the highest resonance shift as strain increases, indicating it is the most sensitive mode. The lower modes (Mode 1, Mode 2, etc.) have smaller shifts, meaning they are less affected by strain. Mode 1 (red line) appears to slightly decrease initially, indicating a possible negative shift before following an increasing trend. Most modes exhibit a nearly trend, meaning the resonance shift increases proportionally with strain. Higer modes have a greater slope, indicating they are more sensitive to strain changes. This graph suggests that higher – order resonance modes in an LPG sensors are more responsive to axial strain.
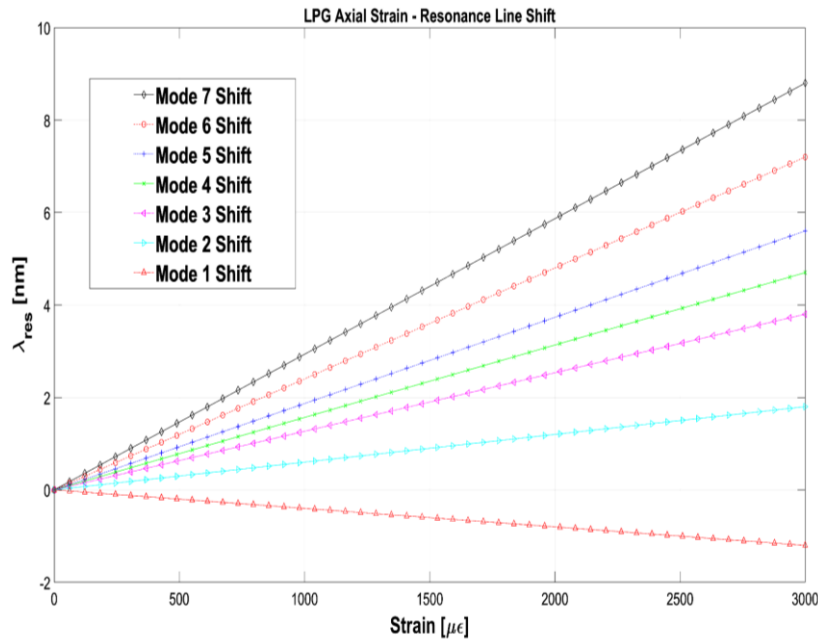
Fig. 6. Spectral shifts of Modes 1 to 7 absorption band peaks (colour online)

The graph 7 represents the effects of axial strain on resonance line shifts in a LPG system. Most mode show an increasing trend in shift with strain. Some shifts are negative, indicating a decrease in resonance for certain modes. Modes 7 Shift Plane Z has the steepest positive sensitive to strain. Some lower order modes (e.g. Mode 1 Shift Plane x) show a downward trend, indicating a negative shift with increasing strain. Thus, different modes respond differently to strain, suggesting they utility in strain sensing applications. The presence of shift planes X and Z suggests anisotropic behavior, meaning the strain response differs depending on the axis of measurement.
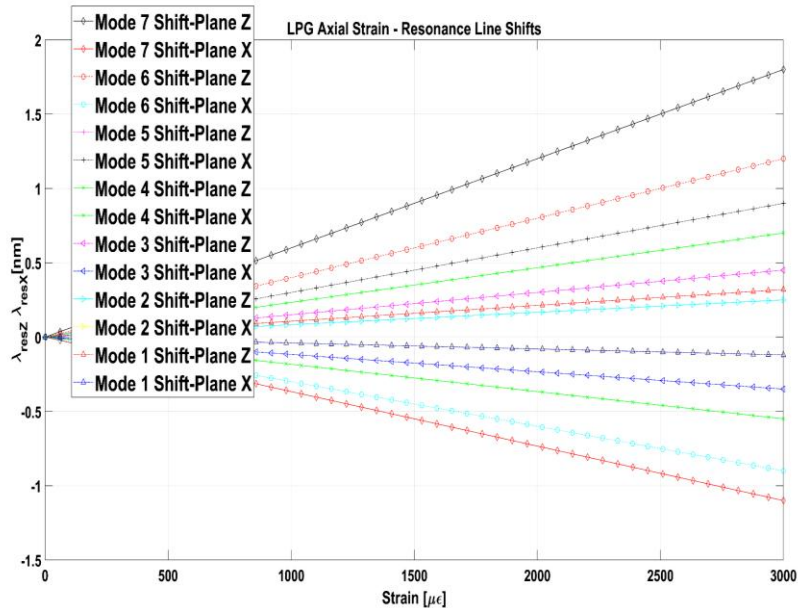
Fig. 7. Effects of axial strain on resonance line shifts in a LPG system (colour online)

4. Conclusions

Graphene coated fibre optic sensors represent a highly promising instrument for health monitoring of composite structures due to their exceptional mechanical properties, sensitivity, and durability. Whether it's strain sensing, temperature monitoring, crack detection, or environmental sensing, these sensors offer critical insights into the integrity of composite materials, helping to enhance the safety, performance, and lifespan of structures in various industries such as aerospace, civil engineering, automotive, and energy. In this paper, we have presented the results obtained in the simulation of health monitoring of composite structures using long-term network fibre sensors. These results are obtained using a finite element method simulation model.

The results shown are of level 1st simulations using long-range network fibre sensors embedded in the composite polymer matrix. Also, these results are intended as a tool for long-range network fibre sensors depending on the materials, parts and devices available to the designer.

Acknowledgements

References

[1] C. Soutis, Prog. Aerosp Sci. **41**(2), 143 (2005).
[2] I. Lancranjan, D. Savastru, S. Miclos, J. Optoelectron. Adv. M. **12**(8), 1636 (2010).
[3] D. Savastru, V. Savu, M. Rusu, M. Tautan, Al. Stanciu, J. Optoelectron. Adv. M. **26**(7-8), 316 (2024).
[4] C. R. Farrar, K. Worden, Phil. Trans. R. Soc. A **365** 303 (2007).
[5] W. Li, S. Guo, Composites Communications **33**, art. number 101213 (2022).
[6] M. Demetgul, V. Y. Senyurek, R. Uyandik, Measurement **69**, 42 (2015).
[7] N. Forintos, T. Sarkadi, T. Czigany, Composites Communications **28**, 100913 (2021).
[8] Y. Yu, X. Liu, J. Li, Yishou Wang, Xinlin Qing, Smart Materials and Structures **31**(1), 015033 (2021).
[9] M. Lin, S. Guo, S. He, W. Li, D. Yang, Composite Structures **286**, 115305 (2022).
[10] K. Gurpreet, S. Rajandeep, S. Aaradhya, K. Harmanpreet Kaur, Optoelectron. Adv. Mat. **17**(5-6), 219 (2023).
[11] Q. Tao, C. Wu, X. Wang, Y. Song, C. Wang, J. Cheng, D. Liu, B. Lu, Optoelectron. Adv. Mat. **18**(3-4), 103 (2024).
[12] K. Chethana, Somesh Nandi, A. P. Guruprasad, S. Ashokan, Recent Advances in Civil Engineering for Sustainable Communities, 167-176, 2024.
[13] M. Aleksey, K. Andrejs, C. Andris, A. Safonovs, Sensors **23**(6), 3327 (2023).
[14] Yu Zhang, Yu Feng, Xiaobo Rui, Lixin Xu, Lei Qi, Zi Yang, Cong Hu, Peng Liu, Haijiang Zhang, Sensors **23**(6), 3052 (2023).
[15] B. Degamber, G. F. Fernando, MRS Bulletin **27**(5), 370 (2002).
[16] K. Bocz, D. Simon, T. Bárány, G. Marosi, Polymers **8**, 289 (2016).
[17] K. Dobrovszky, F. Ronkay, Polymer-Plastics Technology and Engineering **56**(11), 1147 (2017).
[18] J. K. Lee, J. K. Gillham, J. Appl. Polym. Sci. **90**(10), 2665 (2003).
[19] M. A. El-Sherif, J. Radhakrishnan, Journal of Reinforced Plastic and Composites **16**(2), 144 (1997).
[20] J. H. L. Grave, M. L. Håheim, A. T. Echtermeyer, Composites Part B **74**, 138 (2015).
[21] S. W. James, R. P. Tatam, Meas. Sci. Technol. **14**(5), R49 (2003).
[22] A. M. Vengsarkar, P. J. Lemaire, J. B. Judkins, V. Bhatia, T. Erdogan, J. E. Sipe, J. Lightwave Technol. **14**(1), 58 (1996).
[23] T. Erdogan, J. Opt. Soc. Am. A **14**(8), 1760 (1997).
[24] A. Groza, A. Surmeian, C. Diplasu, P. Chapon, D. Manaila-Maximean, M. Ganciu, UPB Sci. Bull. – Series A-Applied Mathematics and Physics **73**(3), 133 (2011).
[25] A. Surmeian, D. Manaila-Maximean, B. Mihalcea, O. Stoican, B. Butoi, O. Danila, P. Dinca, I. Barbut, L. Tudor, A. Fazacas, E. Diplasu, UPB Sci. Bull. -Series A-Applied Mathematics and Physics **77**(4), 273 (2015).
[26] D. Savastru, R. Savastru, I. I. Lancranjan, S. Miclos, Composite Structures **218**, 15 (2019).
[27] M. Rusu, Dan Savastru, V. Savu, Al. Stanciu, M. Tautan, U.P.B. Sci. Bull., Series A **86**(4), 159 (2024).
[28] V. B. Mohana, Kin-tak Laub, D. Huic, D. Bhattacharyya, Composites Part B **142**, 200 (2018).
[29] W. Hu, Y. Huang, C. Chen, Y. Liu, T. Guo, Bai-Ou Guan, Sensors and Actuators B: Chemical **264**, 440 (2018).
[30] A. Popescu, D. Savastru, Al. Stanciu, J. Optoelectron. Adv. M. **26**(7-8), 264 (2024).
[31] S. Miclos, D. Savastru, R. Savastru, I. Lancranjan, Composite Structures **183**, 521 (2018).
[32] G. Vasile, A. Popescu, M. Stafe, S. A. Koziukhin, Dan Savastru, S. Dontu, L. Baschir, V. Sava, B. Chiricuta, M. Mihailescu, C. Negutu, N. Puscas, UPB Sci. Bull. Series A **75**(4), 311 (2013).
[33] Z. Wang, J. R. Heflin, Rogers H. Stolen, Siddharth Ramachandran, Optics Express **13**(8), 2808 (2005).
[34] V. Grubsky, J. Feinberg, Optical Letters **25**, 203 (2000).
[35] X. Shu, L. Zhang, I. Bennion, Journal of Lightwave Technology **20**(2), 255 (2002).
[36] D. Savastru, M. Tautan, V. Savu, Al. Stanciu, M. Rusu, U.P.B. Sci. Bull., Series A **86**(3), 145 (2024).
[37] S. Miclos, L. Baschir, D. Savastru, R. Savastru, I. I. Lancranjan, Composite Structures **256**, 113062 (2021).
[38] D. Savastru, S. Miclos, R. Savastru, I. Lancranjan, Composite Structures **183**, 682 (2018).

*Corresponding author: simona.dontu@inoe.ro